Available online at www.sciencedirect.com

ScienceDirect

Ceramics International 40 (2014) 2655–2661

CERAMICS INTERNATIONAL

www.elsevier.com/locate/ceramint

Effect of lithium extraction on the stabilities, electrochemical properties, and bonding characteristics of $LiFePO_4$ cathode materials: A first-principles investigation

Zhi-Chao Xiong[a], Ying Xie[a,*], Ting-Feng Yi[b,**], Hai-tao Yu[a], Yan-Rong Zhu[b], Yuan-Yuan Zeng[a]

[a]*Key Laboratory of Functional Inorganic Material Chemistry, Ministry of Education, School of Chemistry and Materials Science, Heilongjiang University, Harbin 150080, PR China*

[b]*School of Chemistry and Chemical Engineering, Anhui University of Technology, Maanshan, Anhui 243002, PR China*

Received 11 September 2013; received in revised form 14 October 2013; accepted 14 October 2013
Available online 21 October 2013

Abstract

The impact of lithium extraction on the structural stabilities, electronic structures, bonding characteristics, and electrochemical performances of $LiFePO_4$ compound was investigated by first-principles technique. The results demonstrated that the partition scheme of electrons not only affects the calculated atomic charges but also the magnetic properties. In $FePO_4$ and $LiFePO_4$ compounds, all Fe ions take high spin arrangements and have large magnetic moments (MMs), while the MMs of other ions are very small. The magnetisms of Li_xFePO_4 compounds are mainly originated form Fe ions. It was found that the changes in d band electrons of the transition metals do play an important role in determining the voltage of a battery (versus Li/Li^+). Furthermore, the variations in d band electrons also provide us a method to control the density of states (DOS) and carrier concentration at the Fermi energy. Our calculations confirmed that the substitution of Fe by Co and Ni ions leads to a voltage increase by about 0.70 V and 1.23 V respectively. According to the bond populations, it can be identified that strong covalent bonds are formed between O and P ions. The P–O bonds are much stronger than Fe–O ones. The partial DOSs further revealed that the covalent bonds in Li_xFePO_4 are derived from the orbital overlaps between $O_{2s,2p}$ and $P_{3s,3p}$ states, and the overlap between Fe_{3d} and O_{2p} states. Such covalent bonds are of particularly importance for the excellent thermodynamic stabilities of the two-ends structures of Li_xFePO_4.

Keywords: Lithium-ion battery; Positive-electrode material; $LiFePO_4$; Density functional theory

1. Introduction

Because of their high energy density, rechargeable Li-ion batteries have been considered as one of the most promising energy storage systems in hybrid electric vehicles (HEVs), plug-in hybrid electric vehicles (PHEVs), and full electric vehicles (EVs) among the currently available energy storage technologies [1,2]. Safety and cost are two critical issues and have prevented lithium-ion batteries from being used for power battery. Consequently, a strong research effort has been focused on developing cheaper, safer, more stable, higher energy, and higher power cathode material to replace the conventional $LiCoO_2$. Lithium iron phosphate ($LiFePO_4$), proposed by Padhi et al. [3] in 1997 as a new class of cathode materials, has the potential to enable the production of power batteries, which is becoming a reality. $LiFePO_4$ is an excellent candidate for EV and HEV applications, because it has several advantages over conventional cathodes, such as lower cost, improved safety performance, lower toxicity, and an extremely flat charge–discharge profile at reasonably high potential (3.45 V, versus Li/Li^+) [4,5]. However, $LiFePO_4$ suffers from both poor electronic and ionic conducting properties [6,7]. Therefore, $LiFePO_4$ powders must either be nano-scaled [8,9] or be modified by doping or coating [10–14]. Generally, the research methods for cathode materials usually include

*Corresponding author. Tel./fax: +86 451 86608545.
**Corresponding author.
E-mail addresses: xieying@hlju.edu.cn (Y. Xie), tfyihit@163.com (T.-F. Yi).

0272-8842/$ - see front matter © 2013 Elsevier Ltd and Techna Group S.r.l. All rights reserved.
http://dx.doi.org/10.1016/j.ceramint.2013.10.059

experimental and theoretical techniques. The experimental technique, which is mainly focused on the synthesis–structure–property relation, has certain disadvantages, since it is time or labor consuming and not very efficient due to numerous possible chemistries. However, the introduction of first-principles calculation, which allows us to predict the properties of materials by solving the basic equations of quantum mechanics and statistical mechanics [15], will make it possible to understand the properties of materials prior to synthesis. Liu et al. [16] have calculated the activation energy for Li diffusion in olivine-type $LiFePO_4$ and $FePO_4$. Shi et al. [17] proposed two possible mechanisms to explain the enhanced conduction of $LiFePO_4$. Ouyang et al. [18] pointed out that Li^+ will diffuse along b axis of $LiFePO_4$ based on first-principles predictions. According to the cleavage energies, Shi et al. [19] have reported that the (010) surface of $LiFePO_4$ is more stable than (001) and (100) surfaces. These theoretical investigations have provided us some useful insights into the physical and chemical properties of materials at a microscopic level. As the structure–performance relationship of a cathode material is rather important for subsequent material modification and design, it is the aim of the present work to characterize the impact of Li^+ extraction on the stabilities, electrochemical properties, and bonding properties of $LiFePO_4$ compound from first-principles calculation.

2. Theoretical and computational details

The present calculations were performed within the density functional theory framework [20] implemented in the CASTEP package [21]. The exchange–correlation energies were treated by the Perdew–Wang functional in the Generalized Gradient Approximation form (GGA-PW91) [22]. To deal with the strong-correlated system, a Hubbard U parameter was introduced. The plane-wave energy cutoff used in the calculation was 380.0 eV, and the sampling over Brillouin Zone (BZ) was treated by a $(2 \times 4 \times 5)$ Monkhorst–Pack mesh. This set of parameters guarantees that the total energy of the system can be accurately evaluated, and the energy convergence is within 5.0×10^{-7} eV atom^{-1}.

The calculation model of olivine-type $LiFePO_4$ is shown in Fig. 1. Its space group is P_{mna}, and the conventional cell contains four formula units. O ions are located in a slightly distorted, hexagonal close-packed sites. Li and Fe ions are located in octahedral 4a and 4c sites respectively, while P ions are located in tetrahedral sites. Each FeO_6 octahedron is linked with other two FeO_6 octahedrons through a common vertex in the *b*–*c* plane, forming zigzag chains. Each PO_4 tetrahedron shares a common edge with one FeO_6 octahedron and connects two FeO_6 octahedrons through common vertexes. Li ions form one dimensional chain along the [010] direction of the host structure. In consideration of the magnetic nature of Fe ions, spin polarization was introduced in the calculations. Furthermore, Broyden–Fletcher–Goldfarb–Shanno (BFGS) algorithm [23] was applied to optimize the geometries of Li_xFePO_4. The optimization process was repeated until the average force on the atoms was less than 0.05 eV Å^{-1} and the energy change less than 5.0×10^{-6} eV · atom^{-1}. The optimized lattice constants along a, b, and c axes were determined to be 10.34, 6.03, and 4.73 Å for $LiFePO_4$ and 9.95, 5.99, and 4.90 Å for $FePO_4$.

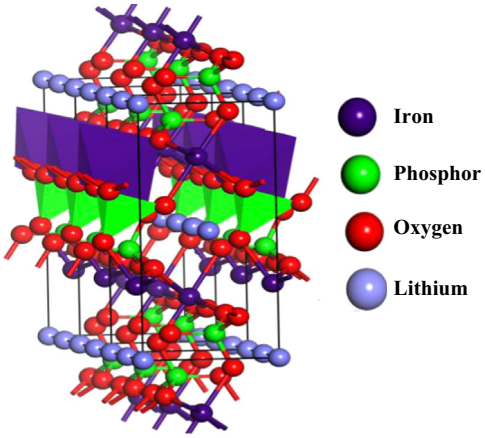

Fig. 1. Computation model of olivine-type $LiFePO_4$.

Table 1
Mülliken atomic populations (in e) for Li_xFePO4 (x=0,1) compounds.

	Fe	Li	P	OI	OII	OIII	OIV
$FePO_4$	1.450	–	2.280	−0.930	−0.930	−0.940	−0.940
$LiFePO_4$	0.970	1.020	2.150	−1.000	−1.000	−1.070	−1.080
Δe	0.48	–	0.13	0.07	0.07	0.13	0.13

3. Results and discussion

The atomic populations of Li_xFePO_4(x=0,1) compounds are given in Table 1 and Fig. 2. After Li^+ intercalation, additional electrons would transfer from the anode to the cathode material through the external circuit to retain the electronic neutrality condition. By comparison of the charge variations, it can be identified the electric behaviors of the materials. According to Table 1, it can be seen that the charge of lithium is +1.02 e, which indicates that Li is a pure ion. Furthermore, along with the intercalation of Li^+, the electrons mentioned above are found to be distributed mainly on the FeO_6 octahedrons, leading to the reductions of Fe and O ions. Usually in experiments, it is believed that the valance of oxygen in Li_xFePO_4 is constant (2^-) and kept unchanged during the charging and discharging processes. However, the host structure of the electrode materials often contains covalent bonds, and determination of the ownership of the electrons that localized at the covalent bonds is a rather delicate task. According to the molecular orbital (MO) theory, the overlap populations can be divided in term of the contributions of atomic orbitals to the occupied bonding states. This is the reason why the charges of oxygen can be changed during the Li^+ intercalation. It should be noted that the partition scheme of electrons not only affects the calculated atomic charges but also the magnetic properties, as discussed later.

The data listed in Table 1 also showed that the charges of oxygen is different, i.e. −0.93 e and −0.94 e in $FePO_4$

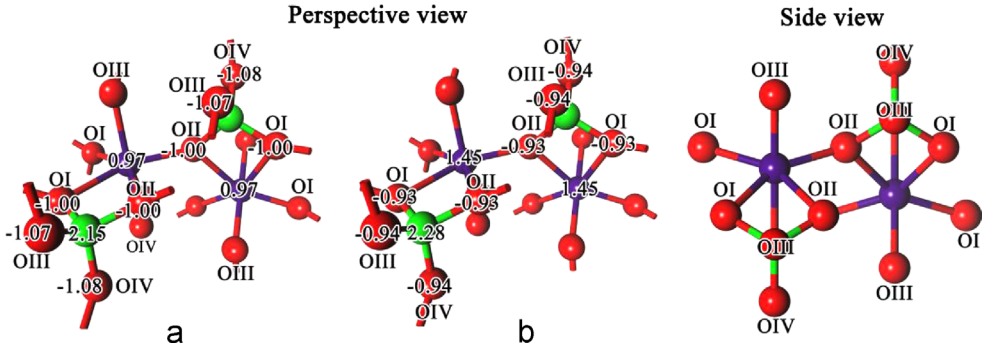

Fig. 2. Atomic populations of Li_xFePO_4 systems (a) $x=1$; (b) $x=0$. The bridge site oxygens that connecting Fe and P ions are triple coordinated and denote as OI and OII, while the double coordinated oxygens are labeled as OIII and OIV.

vs −1.00 e and −1.07 e in $LiFePO_4$. Due to different chemical environments, the oxygen ions are divided into two classes. The first one (OI, OII) is triple coordinated and consists of the shared edge of FeO_6 octahedron and PO_4 tetrahedron, while the later one (OIII, OIV) is double coordinated and is shared vertex of FeO_6 octahedron and PO_4 tetrahedron, as showed in Fig. 2. Similarly, the covalent bonds between P and O ions are also expected, and this behavior results in the charge variations of P species ($\Delta e=0.13$ e) during Li^+ intercalation. Although the partition of electrons at covalent bonds can slightly alter the atomic charges of ions, the Mülliken charge of Fe is greatly reduced ($\Delta e=0.48$ e) during the discharging process. Fe sites can still be regarded as the active redox center. The charge-discharge capacity of $LiFePO_4$ is based on the reaction, $\overset{+2}{Li}\overset{+2}{Fe}PO_4 \underset{\text{Discharge}}{\overset{\text{Charge}}{\rightleftarrows}} \overset{+3}{Fe}PO_4 + Li^+ + e$, which is consistent with experimental results [24,25].

To further analyze the effect of Li^+ intercalation on the bonding characteristics of systems and deduce the experimental valence for Fe ions, further computations are performed. Fig. 3 shows the total density of states (TDOSs) of $FePO_4$. A gap of about 1.24 eV is observed between the occupied valence states and the unoccupied conduction states. This result suggested that the electrical conductivity of $FePO_4$ is poor. It should be noted that the strong correlation effects in transition mental oxides are very important, since they significantly affect the electronic properties of the systems. To reveal the effect, we have calculated the PDOSs diagrams without DFT+U correction, and the result showed that 3d states of Fe are more delocalized, and the band gap for $FePO_4$ is reduced to 0.83 eV. Furthermore, to further examine the atomic interactions in detail, the TDOSs were decomposed according to the contributions of each species, and the results were depicted in Fig. 4. For phosphorus, P_{3s} and P_{3p} states are spread over several energy intervals, i.e. [−21.1 eV, −17.5 eV], [−8.9 eV, −0.39 eV], and [6.48 eV, 15.0 eV], respectively. This feature indicated P_{3s} and P_{3p} states will take sp^3 hybridization, and the highly delocalized nature further implied the formations of certain chemical bonds around phosphorus sphere. For oxygen, it can be found that O_{2s} and O_{2p} states not only overlap strongly with P_{3s} and P_{3p} ones below Fermi energy (0.0 eV), but they also have considerable contributions

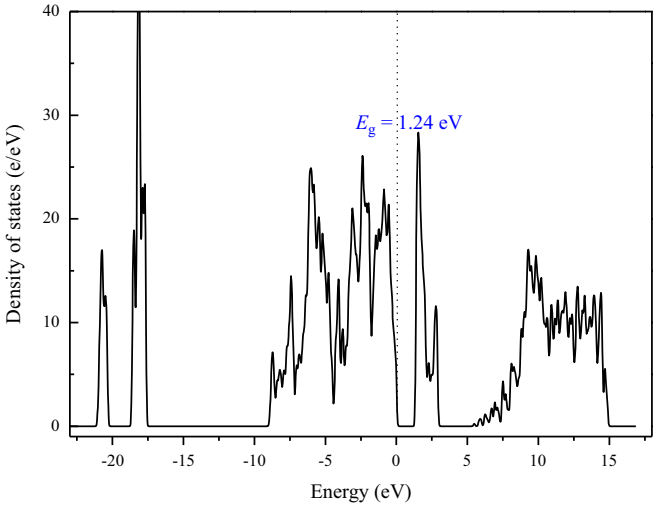

Fig. 3. Total density of states of $FePO_4$ system.

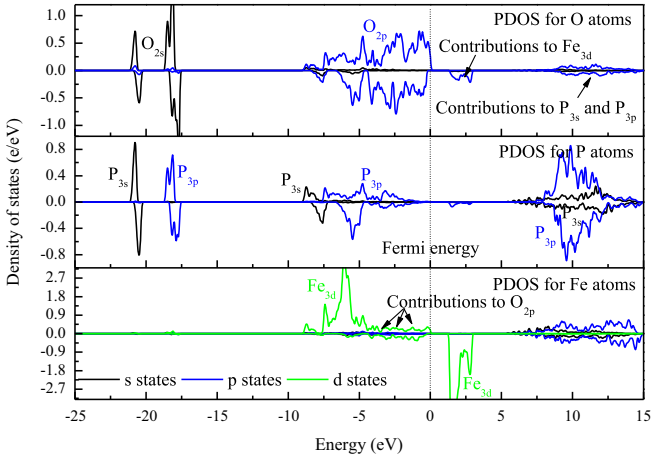

Fig. 4. Partial density of states of all elements in $FePO_4$ system.

to the main DOSs peak of P_{3s} and P_{3p} states located above the Fermi energy. Such a resonant nature identified the existent of $P_{3s,3p}$–O_{2s} and $P_{3s,3p}$–O_{2p} covalent bonds in the compound. Furthermore, it should be emphasized that the DOSs position of P ions with respect to that of O ions is important for the electrochemical performance of the material. It is well known

that the open-circuit voltage ($V_{oc}=(\mu_A-\mu_C)/e$) depends on the electrochemical potentials of the anode (μ_A) and cathode (μ_C) materials. However, for the anode materials, their chemical potentials are usually a little bit smaller than that of metal lithium (upper limit). In order to improve V_{oc}, the only left choice is to reduce μ_C according to specific needs. It has been reported that the chemical potential of cathode is pinned by the top of the anion-p bands of the compound [26], that is to say the top of the O_{2p} bands at the present case. As the main DOSs peak of P_{3s} and P_{3p} states in $FePO_4$ is located at higher energy position than the O_{2p} states, the electron transfer from phosphorus to oxygen (see Table 1) thus allows the O_{2p} states to shift leftward, leading to the decrease of μ_C. Therefore, in comparison to other simple metal oxide cathode materials, the introduction of counter cation (P) will be helpful for improving the open-circuits voltage of the batteries (versus Li/Li^+).

Despite of P_{3s} and P_{3p} states, the electronic structures of the transition metal ions can also affect the position of the O_{2p} band. For iron, the PDOS is divided into two spin channels. At the interval of [−9.0, 0.0 eV], the contributions from Fe_{4s} and Fe_{4p} states are almost negligible, while the resonance between Fe_{3d} and O_{2p} states is very obvious. The result indicated that the interaction between $Fe_{4s,4p}$ and O_{2p} states is rather weak, while valid covalent bond is formed between Fe_{3d} and O_{2p} states. Fig. 4 further suggested that the PDOS position of Fe_{3d} states is located between the O_{2p} and $P_{3s,3p}$ ones. This feature is also very important, because the change of d band electrons of the transition metal will make the modulations of the top of O_{2p} bands and therefore the electrochemical potential of the cathode material possible. According to our estimations, when Fe is fully substituted by Co and Ni ions within the same symmetry group, the intercalation voltage (versus Li^+/Li) increases by about 0.70 and 1.23 V respectively. And the experimental results clearly showed that the voltages (versus Li/Li^+) for $LiFePO_4$, $LiCoPO_4$, and $LiNiPO_4$ are 3.5, 4.8, and 5.1 V, respectively [27]. Both of our theoretical and the reported experimental results demonstrated that the variation of d band electrons of the transition metal does play an important role in determining the voltage of a battery. Supposing that the doping effects, bonding characteristics of a system, and the volume changes upon de/lithiation were known according to the quantum chemistry computations, predictions on the capacity, thermal stability, and cycling performance of doped compounds would become available. The relevant theoretical elucidations thus provide us some useful insights into the design of novel $LiFePO_4$-based cathode materials.

As can be noted form Fig. 4, the α and β spins of Fe are no longer equivalent, and their offset leads to the occurrence of magnetism. According to the Pauli principle and the Hund's rule, the transition metal ions in the octahedral field have two possible spin configurations, i.e. high and low spin ones. Which one is more stable depends on the energies of systems. Our computation confirmed that the high spin arrangement is 0.189 eV per formula unit (18.24 kJ mol^{-1}) lower in energy than the low spin one, being consistent with the experimental observation [28]. Moreover, the PDOS in Fig. 4 also confirmed that α spin channel of Fe is fully filled, while the β spin channel of Fe is almost empty except of few contributions to O_{2p} states. To deduce the valence of Fe in $FePO_4$, we have calculated the magnetic moments of all ions, as given in Table 2.

The results showed that the magnetism of $FePO_4$ is mainly originated form Fe ions, while the magnetic moments of other ions are very small. The value for Fe is calculated to be 4.04 μ_b, which is highly coincident with the experiment value (4.15 μ_b) [28]. However, it should be noted that iron in $FePO_4$ is in the +3 oxidation state with a d^5 spin configuration ($t_{2g}^3e_g^2$) [29], and a theoretical value of 5 μ_b is expected. Both of our theoretical and the reported experimental values underestimate the value by over 17%. The discrepancy may be originated from two aspects. The first one may be due to the incomplete extraction of lithium from $LiFePO_4$ during the experimental characterization. The second one may be result from the partition problem of electrons in covalent compounds as discussed above. Because of the orbital overlaps between different ions, *O* and *P* would obtain some small magnetic moments, which are usually neglected in experiments. If these small contributions are taking into consideration, the total magnetic moment of system becomes 4.96 μ_b, being well consistent with the expected theoretical value.

After lithium intercalation, the filling of electrons on the host framework will change the electronic structures and bonding characteristics of the compound. As shown in Fig. 5, a newly formed occupied state appeared at about −0.10 eV, and the PDOS depicted in Fig. 6 further confirmed that this spin-down state belongs to the t_{2g} symmetry. The separation of this

Table 2
Magnetic moment (in μ_b) of each species in Li_xFePO_4 ($x=0$, 1) compounds.

	Fe	Li	P	OI	OII	OIII	OIV	Sum
$FePO_4$	4.04	–	0.00	0.24	0.24	0.22	0.22	5.96
$LiFePO_4$	3.70	−0.02	0.02	0.10	0.10	0.04	0.06	4.00

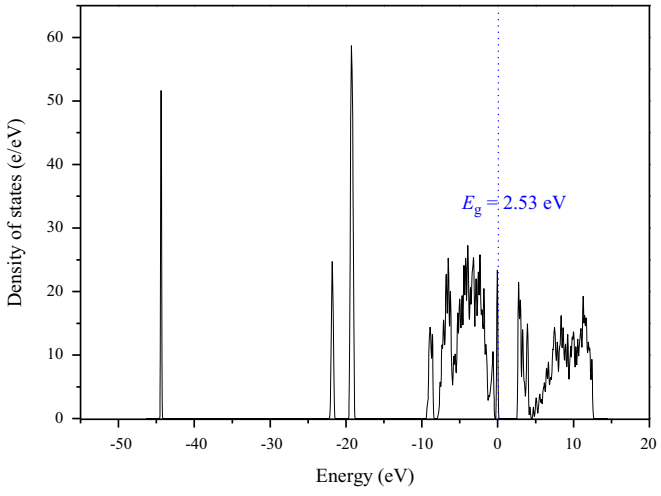

Fig. 5. Total density of states of $LiFePO_4$ system.

particular t_{2g} state from other two t_{2g} states leads to a large band gap (~2.53 eV). For the simulation result without DFT+U correction, the band gap is underestimated to a very large extent, and the relevant value is only about 0.22 eV, which suggested that the strong correlation effect must be explicitly included in the calculations to generate a reasonable result. Furthermore, without DFT+U correction, the calculated total energies of systems are also inaccurate, leading to an underestimated intercalation voltage. In $LiFePO_4$ compound, the calculated magnetic moments for Fe and the whole system are 3.70 and 4.00 μ_b respectively, being consistent with the value for high spin Fe^{2+} ion ($t_{2g}^4e_g^2$) [30,31]. On the basis of the above results, it can be anticipated that partially occupied spin-down t_{2g} band is possible during the discharging process, and this feature may lead to a slight increase of DOS at the Fermi energy and therefore the conductivity of the material. However, once $LiFePO_4$ is formed, the conductance of the system will become even poor. As the conductivity is related to the electronic structure of the system and the d bands of Fe ions in Li_xFePO_4 are dominant near the Fermi energy, it can be expected to improve the intrinsic conductance of $LiFePO_4$-based materials by replacing partial Fe ions with other transition metals. Similar d band structure not only makes the doping feasible but also results in analogous bonding characteristics, while the change of d band electrons may provide us a useful method for modulating the DOS and carrier concentration at the Fermi energy. Such a strategy seems very simple but effective. For example, when lithium extracted from $LiCoPO_4$ to form $CoPO_4$, Co will change from d^7 ($t_{2g}^5e_g^2$) to d^6 ($t_{2g}^4e_g^2$) configuration. Partially filled t_{2g} states are helpful for increasing the density of states at the Fermi energy, and the carrier concentration near Fermi energy may also be enhanced, which is the reason for the significant improvement of conductivity in $LiCo_xFe_{1-x}PO_4$ compounds. This comment can be compared with the reported experimental results [32,33]. Similar to $FePO_4$, the results from Fig. 6 also confirmed the covalent bonds between $P_{3s,3p}$ and $O_{2s,2p}$ orbitals and bonds between Fe_{3d} and O_{2p} ones. Lithium exists mainly in form of ion in $LiFePO_4$ compound, and this existence status of Li is the same as other spinel compounds like $LiMn_2O_4$ [34].

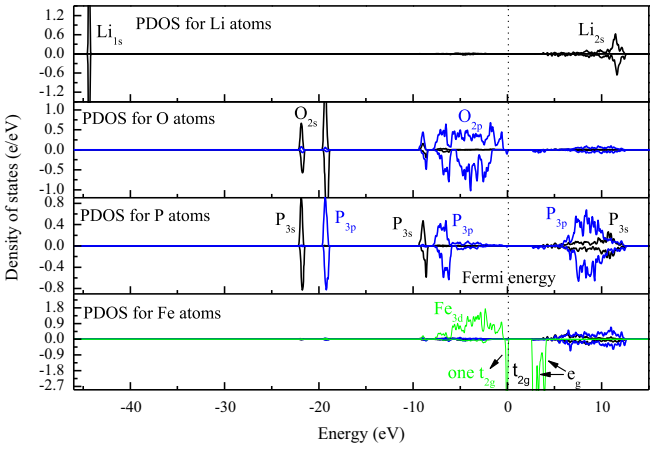

Fig. 6. Partial density of states of all elements in $LiFePO_4$ system.

As the cycling performance of batteries is related to the structural stability of materials, to reveal the effect of chemical bonds we have calculated the electron density differences (EDD) and bond orders. Fig. 7 shows the EDD diagram for $LiFePO_4$. Due to the formation of covalent bonds, the electron distribution is changed. The positive (in blue) or negative (in red) region indicates where the electron density is enriched or depleted respectively. The result showed that the electron density around the oxygen ions significantly increases, while the electron density around the phosphorus and iron ions obviously decreases. It can be concluded that oxygen with negative charge is anion, while phosphorus and iron with positive charge are cations. Moreover, the electron density difference around P ions showed typical sp^3 characteristics,

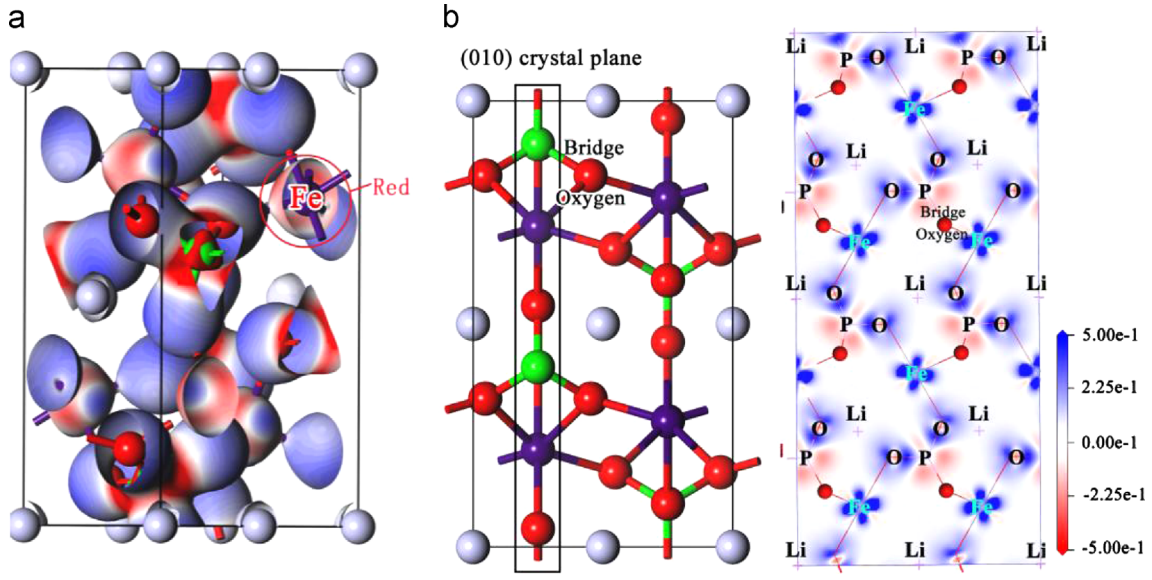

Fig. 7. Electron density difference (EDD) diagram of $LiFePO_4$ crystal. (a) three dimensional view. (b) two dimensional view of (010) crystal plane. The bridge oxygen connecting P and Fe ions is out of the (010) plane and is represented by small red spheres. (For interpretation of the references to color in this figure legend, the reader is referred to the web version of this article.)

Table 3
Bond populations for Li_xFePO_4(x=0, 1) compounds.

	Fe–OI	Fe–OII	Fe–OIII	Fe–OIV	P–OI	P–OIII	Li–O
$FePO_4$	0.13	0.23	0.33	0.35	0.59	0.65	–
$LiFePO_4$	0.12	0.28	0.25	0.25	0.60	0.66	0.01

while those around O and Fe ions displayed explicit p and d orbital characteristics. The results again confirmed that O_{2p} states can effectively overlap with the orbitals of P and Fe ions and then form covalent bonds. To quantitatively illustrate the bond strength, Table 3 gives the bond populations, which are used to assess the covalent or ionic nature of a bond. It should be noted that a value of zero indicates a perfectly ionic bond, while values greater than zero indicate increasing levels of covalency [35].

As can be noted from the table, the P–O bonds (0.60 and 0.66) in $LiFePO_4$ compound are very strong, while the Fe–O bonds are relative weaker (0.12–0.28) in comparison. Such covalent bonds are of particularly importance for the excellent thermal stability of $LiFePO_4$, since the stronger the covalent bonds the more energy will be released due to the formation of bonds [36]. When lithium is extracted from $LiFePO_4$, the bond strength becomes even larger, suggesting that $FePO_4$ compound is also very stable. The very stable two-ends structures during charge and discharge processes indicated that the reversibility of the electrochemical reaction is rather good, leading to excellent cycling performance of batteries. Although the calculations above have confirmed the substitution effect on the intercalation voltage of system, it should be pointed out that the substitution of Fe by other transition metals may also affect the bonding properties of the materials. According to the crystal field theory, the d bands of transition metals (TM) in TMO_6 octahedrons usually exhibit non-bonding or anti-bonding characteristics. Therefore, it can be expected that the substitution of Fe by early 3d/4d transition metals will lead to stronger TM-O bonds but weaker P–O bonds, while the substitution of Fe by late 3d/4d metals may show an opposite trend. However, as the bonding capability of oxygen is determinate and the P-O bonds are rather strong, $LiM_xFe_{1-x}PO_4$ compounds can still retain excellent thermal stabilities. However, the data in Table 3 also suggested an interesting trend that the covalent bonds show anisotropic properties. It can be expected that the weakest chemical bonds in the compounds under external stress/strain would cleave preferentially, leading to the dislocation and mechanical instability of the compound. As proposed by Maxisch [37], the elastic anisotropy of the materials, which is usually related to the microscopic bonding of systems, can lead to the formation of cracks and dislocations within the compounds, leading to the capacity fading of Li_xFePO_4. To reveal the mechanical stabilities and their connections to the microscopic bonding of Li_xMPO_4 electrode materials, urgent investigations are still needed in the future.

4. Conclusions

The electronic structures, bonding characteristics, structural stabilities, and electrochemical performances of $LiFePO_4$ positive electrode material for lithium ion battery were investigated relying on density functional theory (DFT). When electrons transfer to the positive electrode from external circuit, most of them are filled in the Fe ions. The charges of oxygen are slightly changed during the intercalation of Li^+. P_{3s} and P_{3p} states will take sp^3 hybridization, and they overlap with O_{2p} orbits effectively. The introduction of counter cations (P) and the variation of d band electrons of the transition metal are two rather important factors for determining the voltage of a battery. The variation in d band electrons also plays an important role to modulate the DOS and carrier concentration at the Fermi energy, which may be helpful for increasing the conductivity of the compounds. The Fe–O and P–O covalent bonds are of particularly importance to the excellent thermal stability of $FePO_4$ and $LiFePO_4$, well explaining the excellent cycling performance of the cathode.

Using first-principles method to elucidate the microscopic process of lithium intercalation is rather important. The demonstrated achievements in revealing the relationship between the structures and properties during this dynamic process can provide us some important theoretical supports for subsequent experimental synthesis. These capabilities may also establish a valuable tool in the design of new electrode materials for lithium ion battery application.

Acknowledgments

This work was financially supported by the National Natural Science Foundation of China (nos. 21173072, 21301052, and 51274002), the Natural Science Foundation of Heilongjiang Province (no. B201003) and the Program for Innovative Research Team in Anhui University of Technology (no. TD201202).

References

[1] J. Yang, S.-C. Wang, X.-Y. Zhou, J. Xie, Electrochemical behaviors of functionalized carbon nanotubes in $LiPF_6$/EC+DMC electrolyte, Int. J. Electrochem. Sci. 7 (2012) 6118–6126.
[2] C. Dai, Z. Chen, H. Jin, X. Hu, Synthesis and performance of $Li_3(V_{1-x}Mg_x)_2(PO_4)_3$ cathode materials, J. Power Sour. 195 (2010) 5775–5779.
[3] A.K. Padhi, K.S. Nanjundaswamy, J.B. Goodenough, Phospho-olivines as positive-electrode materials for rechargeable lithium batteries, J. Electrochem. Soc. 144 (1997) 1188–1194.
[4] J. Yao, X. Wu, P. Zhang, S. Wei, L. Wang, Effects of Li_2CO_3 as a secondary lithium source on the $LiFePO_4$/C composites prepared via solid-state method, J. Phys. Chem. Solids 73 (2012) 803–807.
[5] W.-J. Zhang, Structure and performance of $LiFePO_4$ cathode materials: a review, J. Power Sour. 196 (2011) 2962–2970.
[6] S.Y. Chung, J.T. Bloking, Y.M. Chiang, Electronically conductive phospho-olivines as lithium storage electrodes, Nat. Mater. 1 (2002) 123–128.
[7] P.P. Prosini, M. Lisi, D. Zane, M. Pasquali, Determination of the chemical diffusion coefficient of lithium in $LiFePO_4$, Solid State Ionics 148 (2002) 45–51.
[8] H. Liu, J. Xie, K Wang, Synthesis and characterization of nano-$LiFePO_4$/carbon composite cathodes from 2-methoxyethanol–water system, J. Alloys Compd. 459 (2008) 521–525.
[9] G. Huang, W. Li, H. Sun, J. Wang, J. Zhang, H. Jiang, F. Zhai, Polyvinylpyrrolidone (PVP) assisted synthesized nano-$LiFePO_4$/C

composite with enhanced low temperature performance, Electrochim. Acta 97 (2013) 92–98.
[10] T.-F. Yi, X.-Y. Li, H. Liu, J. Shu, Y.-R. Zhu, R.-S. Zhu, Recent developments in the doping and surface modification of $LiFePO_4$ as cathode material for power lithium ion battery, Ionics 18 (2012) 529–539.
[11] K.S. Park, A. Benayad, M.S. Park, A. Yamada, S.G. Doo, Tailoring the electrochemical properties of composite electrodes by introducing surface redox-active oxide film: VO_x-impregnated $LiFePO_4$ electrode, Chem. Commun. 46 (2010) 2572–2574.
[12] C.W. Kim, J.S. Park, K.S. Lee, Effect of Fe_2P on the electron conductivity and electrochemical performance of $LiFePO_4$ synthesized by mechanical alloying using Fe^{3+} raw material, J. Power Sour. 163 (2006) 144–150.
[13] C.-Y. Lin, Y.-R. Jhan, J.-G. Duh, Improved capacity and rate capability of Ru-doped and carbon-coated $Li_4Ti_5O_{12}$ anode material, J. Alloys Compd. 509 (2011) 6965–6968.
[14] H. Gao, L. Jiao, J. Yang, Z. Qi, Y. Wang, H. Yuan, High rate capability of Co-doped $LiFePO_4$/C, Electrochim. Acta 97 (2013) 143–149.
[15] G. Ceder, Opportunities and challenges for first-principles materials design and applications to Li battery materials, MRS Bull. 35 (2010) 693–701.
[16] Z. Liu, X. Huang, Factors that affect activation energy for Li diffusion in $LiFePO_4$: a first-principles investigation, Solid State Ionics 181 (2010) 907–913.
[17] S.Q. Shi, L.J. Liu, C.Y. Ouyang, D.S. Wang, Z.X. Wang, L.Q. Chen, X.J. Huang, Enhancement of electronic conductivity of $LiFePO_4$ by Cr doping and its identification by first-principles calculations, Phys. Rev. B 68 (2003) 195108.
[18] C.Y. Ouyang, S.Q. Shi, Z.X. Wang, X.J. Huang, L.Q. Chen, First-principles study of Li ion diffusion in $LiFePO_4$, Phys. Rev. B 69 (2004) 104303.
[19] X. Ouyang, M. Lei, S. Shi, C. Luo, D. Liu, D. Jiang, Z. Ye, M. Lei, First-principles studies on surface electronic structure and stability of LiFePO4, J. Alloys Compds. 476 (2009) 462–465.
[20] P. Hohenberg, W. Kohn, Inhomogeneous electron gas, Phys. Rev. 136 (1964) B864–B871.
[21] M.D. Segall, P.J.D. Lindan, M.J. Probert, C.J. Pickard, P.J. Hasnip, S.J. Clark, M.C. Payne, First-principles simulation: ideas, illustrations and the CASTEP code, J. Phys. Condens. Matter 14 (2002) 2717–2744.
[22] J.P. Perdew, Y. Wang, Accurate and simple analytic representation of the electron–gas correlation energy, Phys. Rev. B 45 (1992) 13244–13249.
[23] T.H. Fischer, J. Almlof, General methods for geometry and wave function optimization, J. Phys. Chem. 96 (1992) 9768–9774.
[24] L.-X. Yuan, Z.-H. Wang, W.-X. Zhang, X.-L. Hu, J.-T. Chen, Y.-H. Huang, John B. Goodenough, Development and challenges of $LiFePO_4$ cathode material for lithium-ion batteries, Energy Environ. Sci. 4 (2011) 269–284.
[25] J.W. Fergus, Recent developments in cathode materials for lithium ion batteries, J. Power Sour. 195 (2010) 939–954.
[26] J.B. Goodenough, K.S. Park, J. Am. Chem. Soc. 135 (2013) 1167–1176.
[27] Z. Gong, Y. Yang, Energy Environ. Sci. 4 (2011) 3223–3342.
[28] G. Rousse, J. Rodriguez-Carvajal, S. Patoux, C. Masquelier, Magnetic structures of the triphylite $LiFePO_4$ and of its delithiated form $FePO_4$, Chem. Mater. 15 (2003) 4082–4090.
[29] M. Yonemura, A. Yamada, Y. Takei, N. Sonoyama, R. Kanno, Comparative kinetic study of olivine Li_xMPO_4 (M=Fe,Mn), J. Electrochem. Soc. 151 (2004) A1352–A1356.
[30] D. Rodic, M. Mitric, R. Tellgren, H. Rundlof, A. Kremenovic, True magnetic structure of the ferrimagnetic garnet $Y_3Fe_5O_{12}$ and magnetic moments of iron ions, J. Magn. Magn. Mater. 191 (1999) 137–145.
[31] P. Léone, G. André, C. Doussier, Y. Moëlo, Neutron diffraction study of the magnetic ordering of jamesonite ($FePb_4Sb_6S_{14}$), J. Magn. Magn. Mater. 284 (2004) 92–96.
[32] H. Gao, L. Jiao, J. Yang, Z. Qi, Y. Wang, H. Yuan, High rate capability of Co-doped $LiFePO_4$/C, Electrochim. Acta 97 (2013) 143–149.
[33] R.-r. Zhao, I.-M. Hung, Y.-T. Li, H.-y. Chen, C.-P. Lin, Synthesis and properties of Co-doped $LiFePO_4$ as cathode material via a hydrothermal route for lithium-ion batteries, J. Alloys Compd. 513 (2012) 282–288.
[34] T.-F. Yi, Y.-R. Zhu, R.-S. Zhu, Density functional theory study of lithium intercalation for 5 V $LiNi_{0.5}Mn_{1.5}O_4$ cathode materials, Solid State Ionics 179 (2008) 2132–2136.
[35] M.D. Segall, R. Shah, C.J. Pickard, M.C. Payne, Population analysis of plane-wave electronic structure calculations of bulk materials, Phys. Rev. B 54 (1996) 16317–16320.
[36] T.-F. Yi, Y. Xie, Y.-R. Zhu, R.-S. Zhu, H. Shen, Structural and thermodynamic stability of $Li_4Ti_5O_{12}$ anode material for lithium-ion battery, J. Power Sour. 222 (2013) 448–454.
[37] T. Maxisch, G. Ceder, Elastic properties of olivine Li_xFePO_4 from first principles, Phys. Rev. B 73 (2006) 174112.